THE ASTROPHYSICAL JOURNAL, 565:1161–1168, 2002 February 1
© 2002. The American Astronomical Society. All rights reserved. Printed in U.S.A.

THE 1998 OUTBURST OF XTE J1550−564: A MODEL BASED ON MULTIWAVELENGTH OBSERVATIONS

K. WU,[1,2] R. SORIA,[1] D. CAMPBELL-WILSON,[2] D. HANNIKAINEN,[3] B. A. HARMON,[4] R. HUNSTEAD,[2] H. JOHNSTON,[2] M. MCCOLLOUGH,[4] AND V. MCINTYRE[2,5]

Received 2001 April 25; accepted 2001 September 13

ABSTRACT

The 1998 September outburst of the black hole X-ray binary XTE J1550−564 was monitored at X-ray, optical, and radio wavelengths. We divide the outburst sequence into five phases and discuss their multiwavelength properties. The outburst starts with a hard X-ray spike, while the soft X-ray flux rises with a longer timescale. We suggest that the onset of the outburst is determined by an increased mass transfer rate from the companion star, but the outburst morphology is determined by the distribution of specific angular momentum in the accreting matter. The companion in XTE J1550−564 is likely to be an active magnetic star, with a surface field strong enough to influence the dynamics of mass transfer. We suggest that its magnetic field can create a magnetic bag capable of confining gas inside the Roche lobe of the primary. The impulsive rise in the hard X-rays is explained by the inflow of material with low angular momentum onto the black hole, on a free-fall timescale, when the magnetic confinement breaks down. At the same time, high angular momentum matter, transferred via ordinary Roche lobe overflow, is responsible for the formation of a disk.

Subject headings: accretion, accretion disks — binaries: close — black hole physics — stars: individual (XTE J1550−564) — stars: magnetic fields — X-rays: stars

On-line material: color figures

1. INTRODUCTION

Many soft X-ray transients (SXTs) are binaries containing a low-mass star transferring material to a black hole. SXT outbursts are usually attributed to accretion disk or mass transfer instabilities and show a variety of patterns and properties. It has been suggested that the companion star may also play an important role, depending on its evolutionary status and its response to irradiative heating. (See, e.g., Tanaka & Lewin 1995 for a review.) The diversity of the outburst behavior in SXTs may therefore arise from the different nature of their companion stars.

XTE J1550−564 was discovered on MJD 51,063 (1998 September 7; MJD = JD−2,400,000.5) by the all-sky monitor (ASM) on board *RXTE* (Smith 1998) and by the Burst and Transient Source Experiment (BATSE) on board *Compton Gamma Ray Observatory* (*CGRO*; Wilson et al. 1998). The optical counterpart was identified shortly afterward (Orosz, Bailyn, & Jain 1998), and a radio source was found at the optical position (Campbell-Wilson et al. 1998). From the optical ellipsoidal modulations, an orbital period of 1.541 ± 0.009 days was inferred (Jain et al. 2001). For a detailed analysis of the X-ray spectral behavior of the source during the 1998 outburst, based on *RXTE* observations, see Sobczak et al. (2000).

[1] Mullard Space Science Laboratory, University College London, Holmbury St. Mary, Dorking, Surrey RH5 6NT, UK; kw@mssl.ucl.ac.uk, rs1@mssl.ucl.ac.uk.

[2] School of Physics, University of Sydney, NSW 2006, Australia.

[3] Department of Physics and Astronomy, University of Southampton, Southampton SO17 1BJ, UK.

[4] NASA Marshall Space Flight Center, SD-50, Huntsville, AL 35812.

[5] Australia Telescope National Facility, CSIRO, P.O. Box 76, Epping, NSW 1710, Australia.

2. X-RAY AND RADIO OBSERVATIONS

The BATSE experiment on board *CGRO* (Fishman et al. 1989) was used to monitor the hard X-ray emission from XTE J1550−564. The BATSE large area detectors (LADs) can monitor the whole sky almost continuously in the energy range of 20 keV to 2 MeV with a typical daily 3 σ sensitivity of better than 100 mcrab. Detector counting rates with a timing resolution of 2.048 s are used for our data analysis. To produce the XTE J1550−564 light curve, single-step occultation data were taken using a standard Earth occultation analysis technique used for monitoring hard X-ray sources (Harmon et al. 1992). Interference from known bright sources was removed. A spectral analysis of the BATSE data indicated that the data were well fitted by a power law with a spectral index of −3.0. The single occultation step data were then fitted with a power law with this index to determine daily flux measurements in the 20–100 keV band.

The initial detection of XTE J1550−564 as a radio source was made on MJD 51,065 with the Molonglo Observatory Synthesis Telescope (MOST) at 843 MHz (Campbell-Wilson et al. 1998). The evolution of the radio source was monitored with MOST over the following 27 days, using partial synthesis observations with integration times ranging from 1 to 9 hr; calibration sources were PKS B1421−490 and B1934−638. Flux density measurements were complicated by sidelobes from the nearby radio-bright supernova remnant G326.3−1.8 (Whiteoak & Green 1996), necessitating an image differencing approach using a matched reference image of the field obtained earlier in 1998 when XTE J1550−564 was quiescent. The flux density estimates are given in Table 1, with the errors being the quadrature combination of a 3 mJy rms noise contribution and a

TABLE 1

MOST Flux Densities for XTE J1550−564 during the 1998 Outburst

Time at Mid-Observation (MJD)	Flux Density at 843 MHz (mJy)
51065.175	12 ± 3
51066.156	16 ± 3
51071.203	27 ± 3
51073.193	18 ± 3
51076.390	168 ± 6
51077.298	327 ± 10
51078.259	375 ± 12
51079.318	221 ± 7
51080.302	155 ± 6
51081.210	120 ± 5
51087.360	20 ± 3
51092.177	14 ± 3

3% calibration uncertainty. Other radio data obtained at higher frequencies with the Australia Telescope Compact Array, together with VLBI images from the Australian Long Baseline Array, will be presented elsewhere (D. Hannikainen et al. 2002, in preparation); preliminary results are given in Hannikainen et al. (2001).

3. THE 1998 OUTBURST SEQUENCE

Figure 1 shows the UV/optical/IR, hard/soft X-ray, and radio light curves of XTE J1550−564 between MJD 51,050 and 51,155. The data in the top panel of Figure 1 are from Jain et al. (1999) and Sanchez-Fernandez et al. (1999). We divide the 1998 outburst into five phases, named after the corresponding stages in the *RXTE*/ASM X-ray light curve (Fig. 1, *bottom panel*): (1) fast rising, (2) slow rising, (3) flare, (4) postflare plateau, and (5) X-ray decline.

Phase 1: fast rise (*MJD 51,063–51,064.5*).—The onset of the outburst is characterized by an impulsive rise in the hard X-rays. The BATSE (20–100 keV) flux reached about 0.3 photons $cm^{-2}\ s^{-1}$ within 1 day and peaked at about 0.4 photons $cm^{-2}\ s^{-1}$ the next day. The *RXTE*/PCA and *RXTE*/HEXTE data (Wilson & Done 2001) show that the 20–200 keV flux peaks at $\approx 1.7 \times 10^{37}$ ergs s^{-1}, and the BATSE data show that the 20–200 keV flux peaks at $\approx 1.8 \times 10^{37}$ ergs s^{-1}, for a distance of 2.5 kpc (Sanchez-Fernandez et al. 1999). Assuming a "canonical" efficiency $\eta \sim 0.1$, the total accreted mass required to account for the initial hard X-ray burst is $\lesssim 10^{23}$ g. In fact, such high values of η are more appropriate for standard disk accretion. Hot advective flows in the inner region, where the hard X-rays are likely to be emitted, are radiatively inefficient, especially if the inflowing matter carries a large radial velocity. For $\eta \sim 10^{-3}$ to 10^{-4} (Quataert & Narayan 1999), the required mass would be 10^{25}–10^{26} g.

The soft X-rays showed an exponential-like rise: the *RXTE*/ASM (2–12 keV) count rate increased from 2 to 40 counts s^{-1}, with an *e*-folding timescale $\lesssim 0.5$ days. The optical brightness reached $(V, I) \approx (16.7, 14.6)$ (Jain et al. 1999), with the possibility that peak brightness had occurred before the optical counterpart was identified. The optical colors were redder than in the other phases, but the X-ray spectrum was harder (Wilson & Done 2001). Archival data from the MOST at 843 MHz showed no obvious detection of radio emission before the outburst.

Phase 2: slow rise (*MJD 51,064.5–51,074*).—This phase can be divided into two stages, (A) MJD 51,064.5–51,068.5 and (B) 51,068.5–51,074, based on the rising timescales of the soft X-rays. The *RXTE*/ASM count rate increased from 40 to 120 counts s^{-1} with an *e*-folding timescale ≈ 3 days in stage A, slowing down markedly through stage B with an *e*-folding timescale $\gtrsim 12$ days. In contrast, the hard X-ray flux dropped rapidly: it had fallen to around half of the phase 1 peak value by the end of stage A (MJD 51,068.5), and remained essentially constant throughout stage B. Table 2 lists the hard and soft X-ray luminosity over phases 1 and 2, inferred from the *RXTE*/PCA data (Wilson & Done 2001), and Table 3 lists the corresponding hard X-ray luminosity deduced from the BATSE data.

TABLE 2

X-Ray Luminosity of XTE J1550−564 during Phases 1 and 2 Deduced from the *RXTE* Data

Observation Date (MJD)	$L_{3-20\ keV}$ (10^{37} ergs s^{-1})	$L_{20-200\ keV}$ (10^{37} ergs s^{-1})	L_{bol} (10^{37} ergs s^{-1})
51063.....	0.67	1.67	3.41
51064.....	0.84	1.57	3.15
51065.....	1.49	1.59	4.41
51067.....	2.24	1.17	5.38
51072.....	2.96	0.83	8.13

Note.—*RXTE*/PCA plus *RXTE*/HEXTE data from Wilson & Done (2001). We assumed a distance of 2.5 kpc (Sanchez-Fernandez et al. 1999).

Radio emission became detectable, with MOST flux densities at a level of 10–30 mJy. Optical emission remained steady, with $(U, B, V, I) \approx (18, 18, 17, 15)$ (Sanchez-Fernandez et al. 1999; Jain et al. 1999).

Phase 3: flare (*MJD 51,074–51,080*).—There was a strong flare in all wavebands. Within 1 day the *RXTE*/ASM count rate rose rapidly from 200 to 500 counts s^{-1}. After peaking on MJD 51,076, it dropped back to the 200 counts s^{-1} level in 1 day and then to 100 counts s^{-1} in another 2 days. The BATSE flux increased almost simultaneously with the soft X-rays, reaching a value of ~ 0.5 photons $cm^{-2}\ s^{-1}$ within a day. It then dropped back to the 0.2 photons $cm^{-2}\ s^{-1}$ level in the next day. Both the *RXTE*/ASM and BATSE

TABLE 3

X-Ray Luminosity of XTE J1550−564 during Phases 1 and 2 Deduced from the BATSE Data

Observation Date (MJD)	$L_{20-100\ keV}$ ($\times 10^{37}$ ergs s^{-1})
51063.438	1.16 ± 0.04
51064.292	1.51 ± 0.05
51064.817	1.75 ± 0.06
51065.453	1.42 ± 0.04
51066.504	1.03 ± 0.04
51067.490	1.01 ± 0.04
51068.475	0.78 ± 0.03
51069.526	0.71 ± 0.02
51070.500	0.78 ± 0.03
51071.276	0.67 ± 0.04
51071.834	0.82 ± 0.04
51072.482	0.85 ± 0.03
51073.501	0.73 ± 0.03
51074.519	0.96 ± 0.03

Note.—We assumed a distance of 2.5 kpc (Sanchez-Fernandez et al. 1999).

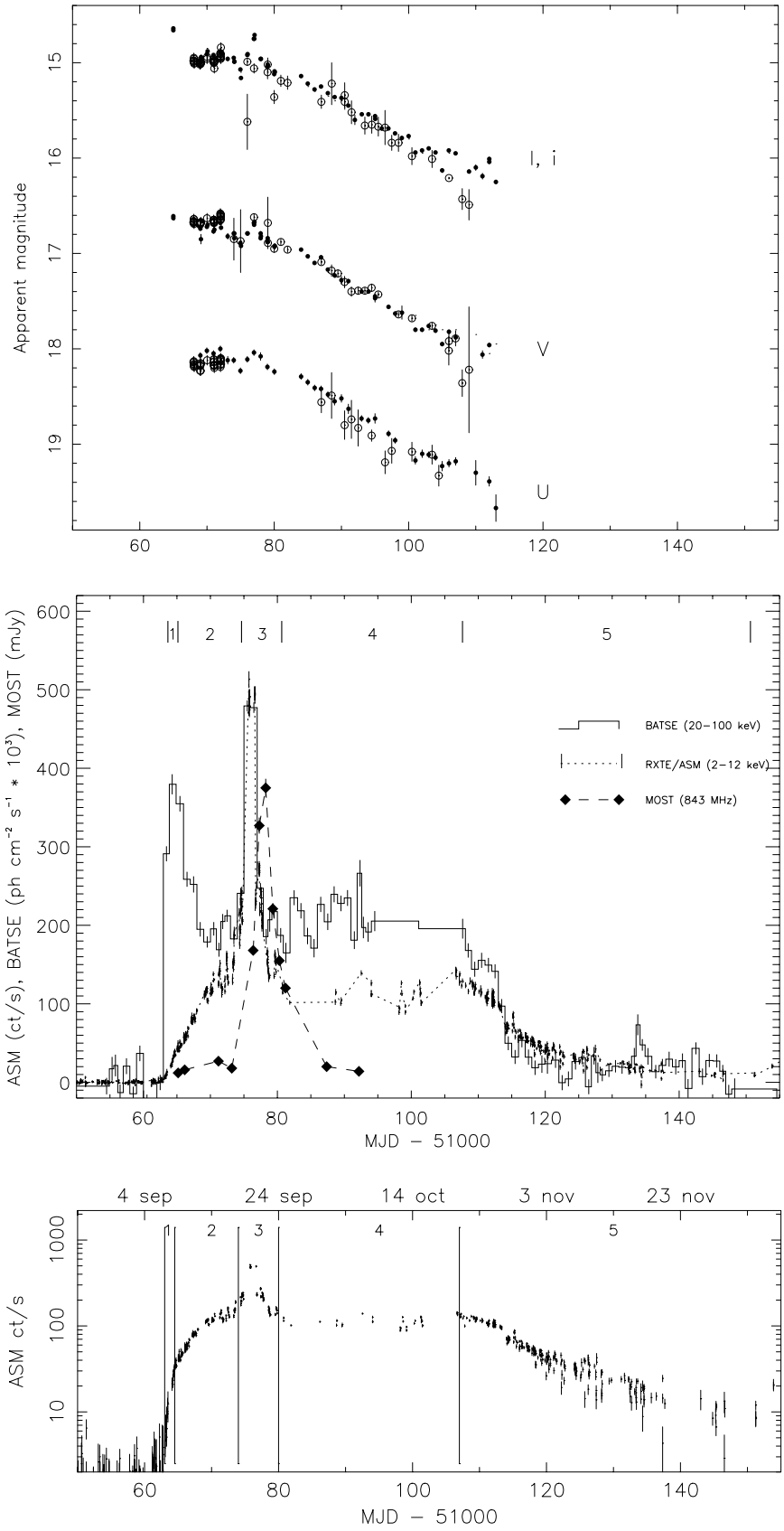

FIG. 1.—*Top*: Optical/IR/UV light curves for the 1998 outburst. Open crcles indicate data from Sanchez-Fernandez et al. (1999); filled circles indicate data from Jain et al. (1999). The upper light curve is in the standard *I* band for the data set of Jain et al. (1999), and in the Gunn *i* band for the data set of Sanchez-Fernandez et al. (1999). The other two light curves are in standard *V* and *U* for both data sets. A possible sharp flare at MJD 51,076 was detected in the *V* band by Sanchez-Fernandez et al. (1999) but was not seen by Jain et al. (1999). *Middle*: X-ray and radio light curves of XTE J1550−564. *Bottom*: Phases of the 1998 outburst sequence shown on a logarithmic plot of the *RXTE*/ASM light curve. [*See the electronic version of the Journal for a color version of this figure.*]

light curves appear to be symmetric with respect to the flare peak in this phase, but differences in the rising and falling times are revealed in higher time-resolution BATSE data.

The radio flare peaked at MJD 51,077.8 $\pm$ 0.1, $\sim$1.8 days after the X-ray peak, with the flux density reaching 380 mJy at 843 MHz. The decay was slower than in the X-ray bands, taking 4 days to decline to the 100 mJy level, which is still about 5 times the preflare flux density. The optical flare showed a delay of $\sim$1 day with respect to the X-ray flare, peaking on MJD 51,077.05; the brightening was less than 0.8 mag in each of the *B*, *V*, and *I* bands. The optical emission reddened during the flare (Jain et al. 1999).

Phase 4: postflare plateau (*MJD 51,080–51,107*).—The *RXTE*/ASM count rate showed some scatter around a mean level of $\sim$120 counts s^{-1}, while the BATSE flux remained steady at the 0.2 photons cm^{-2} s^{-1} level. The 843 MHz flux density continued to decline monotonically, reaching $\sim$14 mJy at MJD 51,092, at which point the monitoring was stopped. The *B*, *V*, and *I* brightness of the source faded steadily by $\approx$0.04 mag day^{-1} (Jain et al. 1999).

Phase 5: X-ray decline (*MJD 51,107–51,150*).—Both the *RXTE*/ASM and the BATSE fluxes declined, with *e*-folding timescales $\approx$11 and 9 days, respectively. The optical brightness of the source continued to fade, with *B* falling below 19.5 mag on MJD 51,113 (Jain et al. 1999).

4. MAGNETIC NATURE OF THE COMPANION STAR

The 1.54 day orbital period together with the faintness of the quiescent optical counterpart suggest that XTE J1550$-$564 is a low-mass system. The companion star should be close to filling its Roche lobe so that the mass transfer can be rapid enough to fuel the outbursts and sustain the subsequent soft state. The mean density of the companion star is therefore $\approx$0.077 g cm^{-3}, similar to that of early B main-sequence stars or G/K subgiants. The quiescent brightness and the observed color differences favor a late-type subgiant.

There are two consequences of having a late-type subgiant companion in the system. First, if we adopt a 1.5 day orbital period and assume that a 10 $M_\odot$ black hole is powering isotropic emission of X-rays at 0.1 of the Eddington luminosity, the fraction of X-ray luminosity ($\sim 10^{36}$ ergs s^{-1}) intercepted by the companion star will be much greater than the intrinsic luminosity of the G/K subgiant companion ($\sim 10^{33}$–10^{35} ergs s^{-1}). Irradiation by soft X-rays will cause surface evaporation and blanketing of the energy diffusing from the stellar interior. Irradiation by hard X-rays will result in the deposition of energy deep in the stellar envelope (e.g., Vilhu, Ergma, & Fedorova 1994). A cool subgiant companion is therefore susceptible to irradiative heating and consequent instabilities.

Second, while the tidally deformed stellar envelope can be locked in synchronous rotation with the orbit, the degenerate stellar core may not attain perfect rotational synchronism. The differential rotation leads to dynamo action and magnetic activity, similar to the situation in the RS CVn systems, which are magnetic close binaries containing a G/K subgiant. For instance, in the well-studied RS CVn system HR 1099, with a 2.8 day orbital period, there is strong evidence (Donati et al. 1992, Vogt et al. 1999) that the K1 IV component harbors a multikilogauss global dipolar field.

Given that fast rotating isolated G/K subgiants (Schrijver & Pols 1993) and G/K subgiants in RS CVn systems are highly magnetically active, G/K subgiants in X-ray binaries can also be magnetic. A surface field strength of 1 kG, corresponding to a magnetic stress of 4×10^4 ergs cm^{-3}, is strong enough to influence the mass- and energy-transport process in the stellar atmosphere.

By postulating a magnetic G/K subgiant companion for XTE J1550$-$564, we are implying a new scenario in which the outburst properties are determined not only by accretion disk instabilities, mass transfer instabilities, and irradiative heating, but also by stellar magnetism.

5. THE PHENOMENOLOGY OF THE OUTBURST

Three remarkable features of the 1998 outburst of XTE J1550$-$564 are (1) an impulsive rise in the hard X-rays while the soft X-ray flux remained low at the onset of the outburst, (2) a subsequent giant flare that occurred almost simultaneously in both hard and soft X-rays about twelve days after the initial rise of the hard X-rays, and (3) an exponential decay in the soft X-ray brightness at the end of phase 5, with the same timescale as those seen in the 1999 and 2000 outbursts.

5.1. *Impulsive Inflow and Hard X-Ray Burst*

It is generally accepted that hard X-ray emission is not thermal emission from an accretion disk (whose maximum temperature is $\sim$1 keV) but is produced by inverse Compton scattering of softer photons off highly energetic ($E \sim 100$ keV) electrons near the black hole. Theoretical studies have shown that accretion of matter with low angular momentum tends to produce hard X-rays (Igumenshchev, Illarionov, & Abramowicz 1999; Beloborodov & Illarionov 2001; Chakrabarti & Titarchuk 1995). The physical justification is that free-falling electrons in a quasi-spherical inflow can acquire kinetic energies $\gtrsim$100 keV as they approach the black hole horizon. The kinetic energy of the infalling electrons powers the Comptonization process, either directly (bulk-motion Comptonization) or after it has been converted into thermal energy (thermal Comptonization).

Impulsive hard X-ray bursts can occur if the injection of material is also impulsive and with a narrow distribution of angular momenta. We therefore argue that an impulsive injection of matter with low angular momentum was responsible for the initial hard X-ray spike in the 1998 outburst and that this initial condition could have been a consequence of a magnetic companion star.

5.2. *Magnetic Bags around G/K Stars*

Extended regions of cool, optically thin, magnetically confined material around a K star are a common feature of RS CVn systems. The typical scale height of these prominences above the photosphere is about twice the stellar radius, implying a volume of $\sim 10^{34}$–10^{35} cm^3 for the confining region. Prominences evolve over timescales of days and contain at any given time a mass of $\sim 10^{20}$ g (Hall & Ramsey 1994).

We argue that the mass of cold, magnetically confined gas can, in fact, be even higher in XTE J1550$-$564, when the magnetic companion star is close to filling its Roche lobe. The inner Lagrangian (L1) point is a saddle point where the gravitational force is negligible, and matter can be more easily lifted up from the photosphere of the companion star. Moreover, the gas is prevented from moving in

any direction other than along the axis between the stars; at the same time, the magnetic field of the companion star restricts the flow along that axis. The gas mass builds up (over a timescale of a few days) until eventually the gas pressure overcomes the magnetic barrier (see Fig. 2 for a cartoon picture of our model).

For magnetic confinement near L1, the magnetic tension/stress must be greater than the gas pressure, implying a critical density for the confined matter:

$$\rho_c \approx \frac{\mu m_H B^2}{8\pi k T} \sim 2 \times 10^{-8} \text{ g cm}^{-3} \left(\frac{B}{1 \text{ kG}}\right)^2 \left(\frac{T}{10^4 \text{ K}}\right)^{-1} . \quad (1)$$

For the sizes of the confining regions in RS CVn systems, and if we assume uniform density, this corresponds to a mass upper limit of $\sim 10^{26}$ g. (If the gas accumulates near the loops' apices, the total mass may be less than this value when the confinement breaks down.) This is consistent with the accreted mass that is required to explain the initial hard X-ray burst (§ 3). By analogy with RS CVn systems, the confined gas in XTE J1550−564 may be located well beyond the L1 point, deep into the Roche lobe of the primary but corotating with the binary. The mass-loss rate of the secondary would then determine the time necessary to fill the magnetic bags.

At the start of an outburst, as the magnetic companion star is close to filling its Roche lobe, part of the photospheric layers is lifted and confined in a magnetic bag beyond the L1 point (low angular momentum component of the accretion flow), while another component starts to be transferred through the Lagrangian point (high angular momentum component). It is the low angular momentum component that we believe is responsible for the peculiar hard X-ray spike seen in phase 1, while the high angular momentum component leads to the formation of the disk.

5.3. *Quasi Free-Fall Accretion*

As the magnetic prominence evolves, the material confined beyond the L1 point tends to collect in the loop apex, until its density increases and it eventually bursts the magnetic dam, breaking free of the field. In a frame corotating with the orbit, the average initial angular momentum of the accreting matter with respect to the black hole is low; i.e., it is effectively in radial free fall. In contrast, the angular momentum of the matter accreted via conventional Roche lobe overflow is large, because the matter passing through the L1 point is transonic, and the accretion stream has a nonzero pitch angle (see Lubow & Shu 1975).

The low angular momentum component of the flow will deviate from near-radial only when approaching the black hole. When the infalling material encounters its centrifugal barrier in the vicinity of the hole, an accretion shock may be formed, converting the kinetic energy to radiation. The photons would then be upscattered by the hot electrons, causing an outburst of hard X-rays. In an alternative scenario, the photons may be upscattered as they interact with the bulk motion of the infalling electrons. When the low angular momentum accreting material is depleted, the quasi-spherical inflow subsides, and the hard X-ray luminosity declines. At the same time, an accretion disk is formed at large radii by the matter transferred via Roche lobe overflow. The steady building and expansion of the disk inward via diffusion processes results in a gradual increase of the optical brightness and then of the soft X-ray luminosity, evident in phases 1 and 2.

The *hard* X-rays can penetrate deep into the star and deposit energy into the convective envelope, thus disturbing the thermal equilibrium of the star. The star must readjust its structure in response to the sudden heating, and it will expand until a new equilibrium is established. At the same time, *soft* X-ray irradiation causes an instantaneous heating of the upper stellar atmosphere and, hence, a rapid increase

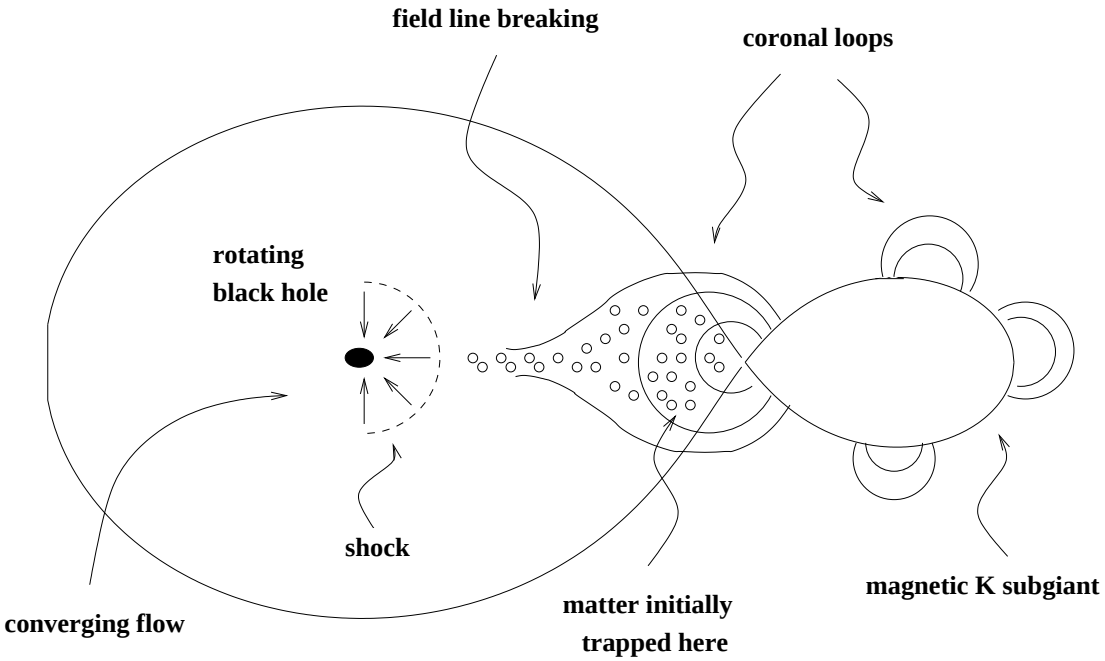

FIG. 2.—Schematic illustration of the magnetic-star model for XTE J1550−564 at the onset of the 1998 outburst. Matter is trapped inside the Roche lobe of the black hole, near the inner Lagrangian point, by the magnetic field of the K subgiant. This provides the initial low angular momentum component of the accretion flow.

in the atmospheric scale height. The timescale for thermal readjustment of the stellar envelope (up to a few weeks) is longer than the dynamic and thermal timescales of atmospheric activity induced by soft X-ray irradiation (Vilhu et al. 1994). Although both hard and soft X-ray irradiation will eventually cause an increase in the rate of mass transfer, there will be a delayed response from the companion star to the initial strong hard X-ray heating. The subsequent onset of a soft state is probably due to the subgiant regaining contact with its critical Roche surface as a result of the delayed expansion caused by the hard X-ray heating.

5.4. *Trigger of the Giant Flare*

During phases 1 and 2 we have accretion of free-falling matter with low angular momentum at small radii, and accretion of matter with high angular momentum, via Roche lobe overflow, at large radii. The former creates a hot, pressure-supported, sub-Keplerian "disk" or quasi-spherical region at small radii, growing outward; the latter creates a Keplerian ring slowly diffusing inward and outward, forming a standard Shakura-Sunyaev disk.

A discontinuity arises when the two accretion flows meet, and the inner boundary of the Keplerian disk is subject to a strong shear. We suggest that this leads to a sudden increase in mass transfer as the outer, denser, colder gas suddenly loses part of its angular momentum at this shear discontinuity, thereby triggering the giant soft and hard X-ray flare around MJD 51,076 (phase 3).

The initial hard X-ray burst in phase 1 and the giant flare in phase 3 have different soft X-ray properties. Moreover, the latter was accompanied by strong radio activity. Because of insufficient shear, the quasi-spherical accretion flow in phase 1 is unlikely to amplify the seed magnetic field carried by the infalling matter significantly. Only after an accretion disk is formed will dynamo action become efficient and amplify the field. One possibility is that when the magnetic disk joins the sub-Keplerian inner region and mass accretion suddenly increases (giant flare), the magnetic field is dragged rapidly toward the black hole event horizon by the accreting matter. The field would be compressed and might reconnect, causing the expulsion of disk material and hence the formation of a radio flare/jet.

The small increase in optical brightness during the giant X-ray flare is surprising. However, the heating of the companion star and of the accretion disk could have saturated owing to strong X-ray irradiation during the previous phases, and the accretion disk may already have been extended to its outer tidal limit.

5.5. *Drainage of the Accretion Disk*

Around MJD 51,110 both the hard and soft X-ray luminosity began to decline exponentially, with the soft X-rays lagging behind the hard. The *e*-folding decay timescale is 11.0 ± 0.1 days for *RXTE*/ASM and slightly shorter for BATSE. The corresponding decay timescales for the later outbursts in 1998/1999 and 2000 are almost identical: 11.3 ± 0.1 and 11.1 ± 0.2 days, respectively (Fig. 3).

The decline in the X-ray luminosity is therefore evidence of the drainage of the accretion disk. The timescale on which a disk is emptied is

$$t \approx \frac{R_d^2}{\nu} \sim \frac{1}{\nu}\left(\frac{0.6}{1+q}\right)^2\left[\left(\frac{P}{2\pi}\right)^2 GM_1(1+q)\right]^{2/3} \qquad (2)$$

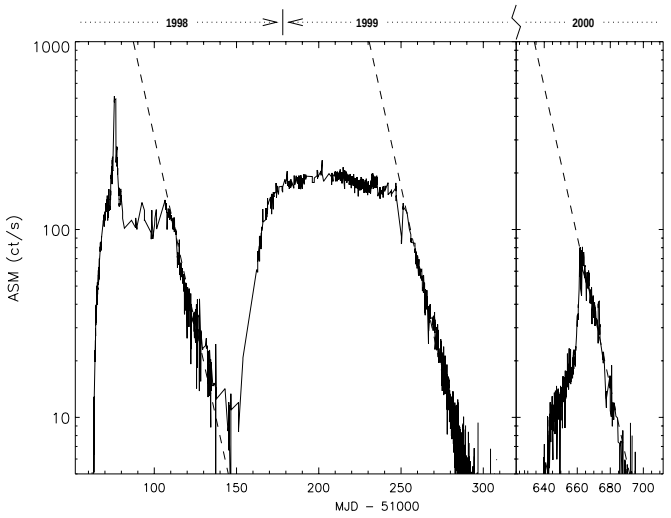

FIG. 3.—*RXTE*/ASM light curves for the three outbursts of XTE J1550−564 between 1998 and 2000. The dashed lines correspond to an exponential decay with an *e*-folding timescale of 11 days.

(Pringle 1981), where G is the gravitational constant, P the orbital period, M_1 the black hole mass, $q(\equiv M_2/M_1)$ the mass ratio, R_d the disk radius, and ν the effective viscosity. A decay timescale of 11 days implies $\nu \sim 2.3 \times 10^{17}$ cm^2 s^{-1} if $q \approx 0.1$, $M_1 = 10\ M_\odot$. The effective viscosity is often expressed in terms of a constant parameter α (Shakura & Sunyaev 1973):

$$\nu \approx \alpha H c_s \approx \alpha c_s^2/\Omega\ , \qquad (3)$$

where the sound speed $c_s \approx (kT/m_p)^{1/2}$ and the Keplerian angular velocity $\Omega \approx 1.2 \times 10^{-3}\ (M/10\ M_\odot)^{1/2}\ (R/10^{11}$ cm$)^{-3/2}$ s^{-1}. For temperatures 10^4 K $\lesssim T \lesssim 10^5$ K, typical of the outer regions of the disk ($R \approx R_d$), the observed timescale corresponds to an effective $\alpha \sim 10$ at large radii.

6. A MODEL FOR THE ONSET OF THE OUTBURSTS

6.1. *A Subclass of Black Hole Candidate Outbursts*

A remarkable characteristic of the outburst behavior of XTE J1550−564 is the presence of a sharp hard X-ray spike during the initial rise. This spectral behavior is different to that observed in systems such as GRO J1655−40, GS 1354−64, or GX 339−4. The 1996 outburst of GRO J1655−40 started with a very soft state (Hynes et al. 1998) and the hard X-rays turned on about a month after the start of the outburst. In GS 1354−64, the soft and hard X-ray fluxes are well correlated during their rise and decline (Brocksopp et al. 2001). In GX 339−4, the soft and hard fluxes tend to be anticorrelated (Corbel et al. 2000). No initial hard X-ray spike is detected in any of those three systems.

In fact, XTE J1550−564 is not the only system showing a hard X-ray spike at the onset of an outburst. XTE J1859+226 (Wood et al. 1999; McCollough & Wilson 1999; Brocksopp et al. 2002) and XTE J2012+381 (Vasiliev, Trudolyubov, & Revnivtsev 2000) are two other good examples. In these three systems, the hard X-ray flux reached a maximum within the first day after detection, and then declined after about 4 days. The soft X-ray flux increased more steadily and at a slower pace, for ~ 10 days.

The similarity in the X-ray spectral properties of XTE J1550−564, XTE J1859+226, and XTE J2012+381 can be

seen from their hardness ratios plots (Fig. 4; data from the public *RXTE*/ASM archive). These systems probably belong to a subclass of black hole transients, sharing a similar physical mechanism that gives rise to a strong hard X-ray spike at the onset of an outburst. A more detailed analysis of the hard X-ray properties of this type of systems will be presented elsewhere (R. Soria et al 2001, in preparation).

6.2. *Formation of the Hard X-Ray Spike*

We propose that the difference between the outburst behavior of systems like XTE J1550−564 and of the other black hole transients is due to the difference in the relative angular momentum content of their accreting matter. Matter accreted via a stellar wind has a lower specific angular momentum than matter accreted via Roche lobe overflow, and it has been suggested that the wind-fed systems and systems with Roche lobe overflow have different preferential spectral states (Beloborodov & Illarionov 2001. There is also evidence that the accretion flow in black hole X-ray binaries consists of separate components, each with a different distribution of angular momentum. Observations of 1E 1740−294, GRS 1758−258, and GX 339−4 (Smith, Heindl, & Swank 2001) indicate that the delay of the soft component relative to the hard component (approximately equal to the difference between the viscous and the free-fall timescale) is more evident for systems with Roche lobe overflow, i.e., those where a large accretion disk is present, and the high angular momentum component dominates. Shorter viscous delays were observed for wind-fed systems (e.g., Cyg X-1 in the hard state; Smith et al. 2001) where the low angular momentum component dominates.

We attribute the presence of the hard X-ray spike in XTE J1550−564 to an inflow of accreting matter with low angular momentum, lasting over the first few days. The 3–200 keV X-ray spectrum of XTE J1550−564 at the peak of the initial hard phase (Wilson & Done 2001) is, in fact, very similar to the spectrum of Cyg X-1 in its hard state, consistent with the interpretation that the initial accretion flow in XTE J1550−564 was dominated by the low angular-momentum component.

6.3. *Outburst Morphology: Role of the Specific Angular Momentum*

The hard and soft states of black hole candidate (BHC) outbursts are usually explained by models invoking an optically thick, geometrically thin accretion disk which is initially truncated in the inner region. The optical/IR flux comes mostly from the outer disk region. The soft X-ray flux rises on a viscous timescale as the disk grows inward at the beginning of the outburst and is therefore delayed with respect to the optical flux. At small radii, the accretion flow is hot and quasi-spherical. The hard X-rays are due to inverse-Compton scattering of soft photons from the disk or the companion star by highly energetic electrons in the hot quasi-spherical flow near the black hole. When the quasi-spherical flow subsides and is replaced by the thin accretion disk extending down toward the innermost stable circular orbit of the black hole, the system is observed in a high/soft state.

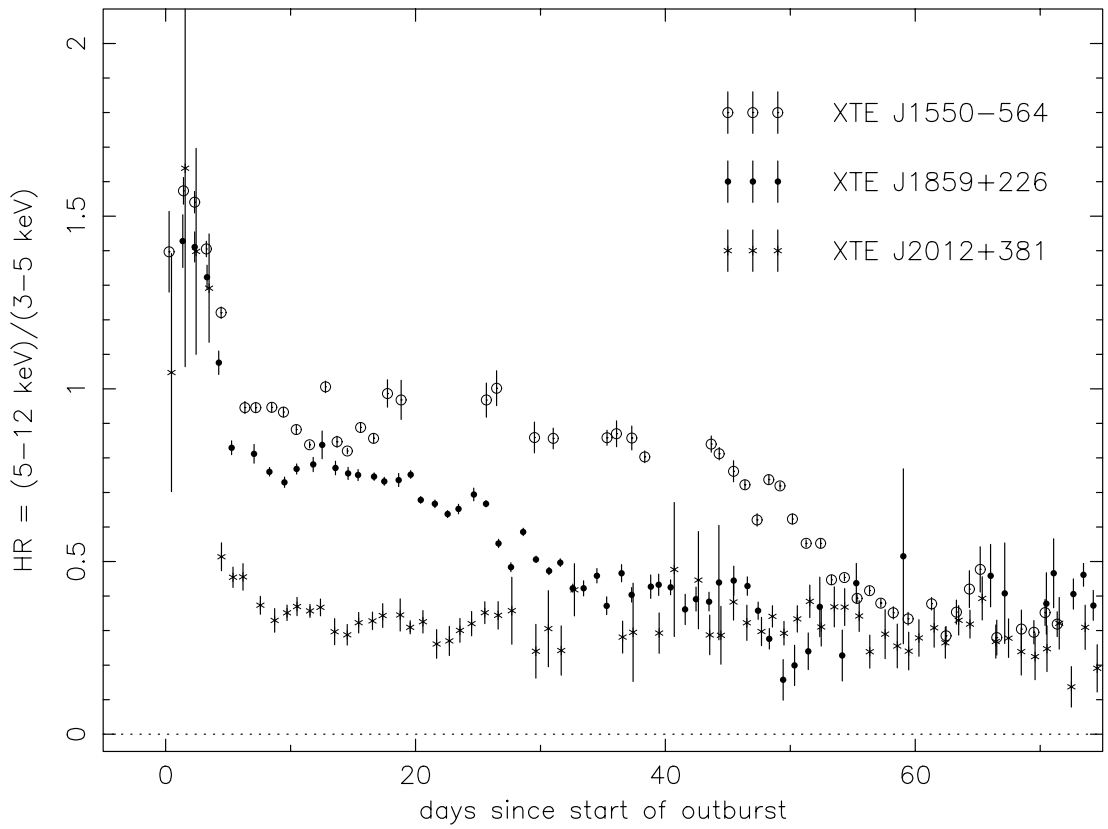

FIG. 4.—Evolution of the *RXTE*/ASM hardness ratios (counts in the 5–12 keV band / counts in the 3–5 keV band) during the outbursts of the BHCs XTE J1550−564 (*open circles*), XTE J1859+226 (*filled circles*), and XTE J2012+381 (*asterisks*). For XTE J1550−564, time = MJD − 50,063; for XTE J1859+226, time = MJD − 51,459; and for XTE J2012+381, time = MJD − 50,956. All three systems show an initial hard spike. [*See the electronic version of the Journal for a color version of this figure.*]

In our model, the outburst behavior is determined by the mass transfer rate (which determines the energetics of the burst) and the angular momentum distribution of the accreting matter (which determines the initial spectral properties and the X-ray rise time). The inner, quasi-spherical flow is fed by the accretion of material with low angular momentum, while the disk is formed by accretion of high angular momentum matter transferred via Roche lobe overflow. The initial hard X-ray emission is caused by a sudden injection of accreting matter with low angular momentum. When the injection ends and the supply of low angular momentum accreting matter is depleted, the hard X-ray flux declines. In the case of XTE J1550−564, we attribute the decline of the low angular momentum accretion flow to the emptying of the magnetic reservoir. After the magnetic bags are drained, accretion proceeds only via Roche lobe overflow.

Our model is in contrast to scenarios based on advection-dominated accretion flows (ADAF models; see Narayan & Yi 1995; Esin, McClintock, & Narayan 1997), in which spectral softening is attributed to the collapse of the hot, quasi-spherical flow into an optically thick disk when the mass accretion rate increases. An application of the ADAF model to the 1998 outburst of XTE J1550−564 has been presented by Wilson & Done (2001). The conventional ADAF scenarios do not explain why in some systems (such as XTE J1550−564) the hot inner region produces a strong hard X-ray spike before collapsing, while in other systems (such as GRO J1655−40) no such initial spike is observed. Moreover, the observed duration of the initial hard emission seems to be much longer than the timescale for the collapse of the hot flow in the conventional ADAF model (Wilson & Done 2001).

7. SUMMARY

We describe the morphology of the 1998 outburst of XTE J1550−564, dividing it into five phases. The outburst starts with a hard X-ray flare (peaking after $\sim$1 day); the same behavior is observed in at least two other BHCs. We propose that the companion star in XTE J1550−564 is magnetically active, and its magnetic field creates a magnetic bag capable of confining $\sim 10^{26}$ g of gas inside the Roche lobe of the primary, corotating with the binary. The impulsive rise in the hard X-rays is explained by the inflow of material with low angular momentum onto the black hole, on a free-fall timescale, when the magnetic confinement breaks down. At the same time, matter with higher angular momentum, transferred via Roche lobe overflow, begins to form a Keplerian disk, responsible for the soft X-rays and optical emission. We suggest that the onset of the outburst is determined by an increased mass transfer rate from the companion star, but the outburst morphology is determined by the distribution of specific angular momentum in the accreting matter. When the inner boundary of the outer, denser Keplerian disk comes into contact with the inner sub-Keplerian hot region, the disk matter is subject to a strong shear and loses angular momentum. This disturbs the stability of the accretion disk, causes a sudden increase in the mass accretion rate, and is responsible for the observed giant X-ray flare and radio ejections. An identical timescale of 11 days is found for the decay of the soft X-ray flux in the three outbursts observed in this system, implying an effective viscosity $\nu \sim 2.3 \times 10^{17}$ cm^2 s^{-1} for the accretion disk.

We thank Celia Sanchez-Fernandez and Raj Jain for allowing us to use their optical data and Colin Wilson for providing helpful information on his X-ray spectral fitting. We also thank the anonymous referee for providing useful suggestions on how to improve our paper. K. W. acknowledges support from the ARC Australian Research Fellowship and the PPARC-MSSL Visiting Fellowship and thanks Phil Charles for funding his visits to the University of Southampton. R. S. acknowledges support from the University of Sydney during his visit there. D. C. H. acknowledges the support of a UK PPARC postdoctoral research grant to the University of Southampton, and financial support from the Academy of Finland, and thanks the Astrophysics Department, Sydney University for hospitality during her visits. MOST is operated by Sydney University and supported by grants from the Australian Research Council.

REFERENCES

Beloborodov, A. M., & Illarionov, A. F. 2001, MNRAS, 323, 167
Brocksopp, C., Jonker, P. G., Fender, R. P., Groot, P. J., van der Klis, M., & Tingay, S. J. 2001, MNRAS, 323, 517
Brocksopp, C., et al. 2002, MNRAS, submitted
Campbell-Wilson, D., McIntyre, V., Hunstead, R. W., & Green, A. 1998, IAU Circ., 7010, 3
Chakrabarti, S., & Titarchuk, L. G. 1995, ApJ, 455, 623
Corbel, S., Fender, R. P., Tzioumis, A. K., Nowak, M., McIntyre, V., Durouchoux, P., & Sood, R. 2000, A&A, 359, 251
Donati, J.-F., et al. 1992, A&A, 265, 682
Esin, A. A., McClintock, J. E., & Narayan, R. 1997, ApJ, 489, 865 (erratum 500, 523)
Fishman, G. J., et al. 1989, in Proc. Gamma-Ray Observatory Science Workshop, ed. W. N. Johnson (Greenbelt: NASA GSFC), 2
Hall, J. C., & Ramsey, L. W. 1994, AJ, 107, 1149
Hannikainen, D. C., et al. 2001, in Proc. 4th INTEGRAL Workshop (Noordwijk: ESA), in press
Harmon, B. A., et al. 1992, in Proc. Compton Observatory Science Workshop, ed. C. R. Shrader, N. Gehrels, & B. Dennis (Washington, DC: NASA), 69
Hynes, R. I., et al. 1998, MNRAS, 300, 64
Igumenshchev, I. V., Illarionov, A. F., & Abramowicz, M. A. 1999, ApJ, 517, L55
Jain, R. K., Bailyn, C. D., Orosz, J. A., McClintock, J. E., Sobczak, G. J., & Remillard, R. A. 2001, ApJ, 546, 1086
Jain, R. K., Bailyn, C. D., Orosz, J. A., Remillard, R. A., & McClintock, J. E. 1999, ApJ, 517, L131
Lubow, S. H., & Shu, F. H. 1975, ApJ, 198, 383
McCollough, M. L., & Wilson, C. A. 1999, IAU Circ., 7282, 3
Narayan, R., & Yi, I. 1995, ApJ, 444, 231
Orosz, J. A., Bailyn, C. D., & Jain, R. K. 1998, IAU Circ., 7009, 1
Pringle, J. E. 1981, ARA&A, 19, 137
Quataert, E., & Narayan, R. 1999, ApJ, 520, 298
Sanchez-Fernandez, C., et al. 1999, A&A, 348, L9
Schrijver, C. J., & Pols, O. R. 1993, A&A, 278, 51
Shakura, N. I., & Sunyaev, R. A. 1973, A&A, 24, 337
Smith, D. A. 1998, IAU Circ., 7008, 1
Smith, D. M., Heindl, W. A., & Swank, J. H. 2001, preprint (astro-ph/0103304)
Sobczak, G. J., McClintock, J. E., Remillard, R. A., Cui, W., Levine, A. M., Morgan, E. H., Orosz, J. A., & Bailyn, C. D. 2000, ApJ, 544, 993
Tanaka, Y., & Lewin, W. H. G. 1995, in X-Ray Binaries, ed. W. H. G. Lewin, J. van Paradijs, & E. P. J. van den Heuvel (Cambridge: Cambridge Univ. Press), 126
Vasiliev, L., Trudolyubov, S., & Revnivtsev, M. 2000, A&A, 362, L53
Vilhu, O., Ergma, E., & Fedorova, A. 1994, A&A, 291, 842
Vogt, S. S., Hatzes, A., Misch, A. A., & Meurster, M. 1999, ApJS, 121, 547
Whiteoak, J. B. Z., & Green, A. J. 1996, A&AS, 118, 329
Wilson, C. D., & Done, C. 2001, MNRAS, 325, 167
Wilson, C. A., Harmon, B. A., Paciesas, W. S., & McCollough, M. L. 1998, IAU Circ., 7010, 2
Wood, A., Smith, D. A., Marshall, F. E., & Swank, J. E. 1999, IAU Circ., 7274, 1